mTORC1 Controls Mitochondrial Activity and Biogenesis through 4E-BP-Dependent Translational Regulation

Masahiro Morita,[1,2] Simon-Pierre Gravel,[1,2] Valérie Chénard,[1,2] Kristina Sikström,[3] Liang Zheng,[4] Tommy Alain,[1,2] Valentina Gandin,[5,7] Daina Avizonis,[2] Meztli Arguello,[1,2] Chadi Zakaria,[1,2] Shannon McLaughlan,[5,7] Yann Nouet,[1,2] Arnim Pause,[1,2] Michael Pollak,[5,6,7] Eyal Gottlieb,[4] Ola Larsson,[3] Julie St-Pierre,[1,2,*] Ivan Topisirovic,[5,7,*] and Nahum Sonenberg[1,2,*]

[1]Department of Biochemistry
[2]Goodman Cancer Research Centre
McGill University, Montreal, QC H3A 1A3, Canada
[3]Department of Oncology-Pathology, Karolinska Institutet, Stockholm, 171 76, Sweden
[4]Cancer Research UK, The Beatson Institute for Cancer Research, Switchback Road, Glasgow G61 1BD, Scotland, UK
[5]Lady Davis Institute for Medical Research
[6]Cancer Prevention Center, Sir Mortimer B. Davis-Jewish General Hospital
McGill University, Montreal, QC H3T 1E2, Canada
[7]Department of Oncology, McGill University, Montreal, QC H2W 1S6, Canada
*Correspondence: julie.st-pierre@mcgill.ca (J.S.-P.), ivan.topisirovic@mcgill.ca (I.T.), nahum.sonenberg@mcgill.ca (N.S.)

SUMMARY

mRNA translation is thought to be the most energy-consuming process in the cell. Translation and energy metabolism are dysregulated in a variety of diseases including cancer, diabetes, and heart disease. However, the mechanisms that coordinate translation and energy metabolism in mammals remain largely unknown. The mechanistic/mammalian target of rapamycin complex 1 (mTORC1) stimulates mRNA translation and other anabolic processes. We demonstrate that mTORC1 controls mitochondrial activity and biogenesis by selectively promoting translation of nucleus-encoded mitochondria-related mRNAs via inhibition of the eukaryotic translation initiation factor 4E (eIF4E)-binding proteins (4E-BPs). Stimulating the translation of nucleus-encoded mitochondria-related mRNAs engenders an increase in ATP production capacity, a required energy source for translation. These findings establish a feed-forward loop that links mRNA translation to oxidative phosphorylation, thereby providing a key mechanism linking aberrant mTOR signaling to conditions of abnormal cellular energy metabolism such as neoplasia and insulin resistance.

INTRODUCTION

Translation is considered to be one of the most energy-consuming cellular processes, accounting for ~20%–30% of total ATP consumption, not including the energy expended during the biosynthesis of rRNA (Buttgereit and Brand, 1995; Rolfe and Brown, 1997). Mitochondria are the main producers of ATP under physiological conditions in mammals and play a critical role in overall energy balance (Vander Heiden et al., 2009).

The mechanistic/mammalian target of rapamycin (mTOR) is a serine/threonine kinase that has been implicated in a variety of physiological processes and pathological states (Zoncu et al., 2011). mTOR forms two distinct complexes, mTOR complex 1 (mTORC1) and 2 (mTORC2), which differ in their composition, downstream targets, regulation, and sensitivity to the allosteric inhibitor rapamycin (Hara et al., 2002; Kim et al., 2002; Sarbassov et al., 2004). mTORC1 stimulates mRNA translation and other anabolic processes (e.g., lipogenesis) in response to a variety of extracellular signals and intracellular cues such as nutrients, oxygen, and hormones (Laplante and Sabatini, 2012; Yecies and Manning, 2011). mTORC2 controls cell survival, cytoskeleton organization (Jacinto et al., 2004; Sarbassov et al., 2004), lipogenesis, and gluconeogenesis (Hagiwara et al., 2012; Yuan et al., 2012) by activating AGC kinases including serum- and glucocorticoid-regulated kinase (SGK) and AKT (García-Martínez and Alessi, 2008; Ikenoue et al., 2008; Sarbassov et al., 2005). Hyperactivation of mTORC1 frequently accompanies diseases characterized by perturbations in energy metabolism and translation including cancer and the metabolic syndrome (Laplante and Sabatini, 2012).

mTORC1 stimulates translation by phosphorylating downstream targets including 4E-BPs and ribosomal protein S6 kinases (S6Ks) (Roux and Topisirovic, 2012). Phosphorylation of 4E-BPs by mTORC1 leads to their dissociation from eIF4E, thereby allowing association of eIF4E with eIF4G and the assembly of the eIF4F translation initiation complex at the mRNA 5′ end (Gingras et al., 1999, 2001; Pause et al., 1994). S6Ks phosphorylate components of the translational machinery and associated factors such as ribosomal protein S6, eIF4B, and PDCD4 (Banerjee et al., 1990; Dorrello et al., 2006; Kozma et al., 1990; Shahbazian et al., 2006). mTORC1 also controls energy metabolism by stimulating the activity of several transcriptional regulators such as PPARγ coactivator-1α (PGC-1α), sterol

regulatory element-binding protein 1/2 (SREBP1/2), and hypoxia inducible factor-1α (HIF-1α) (Cunningham et al., 2007; Düvel et al., 2010; Porstmann et al., 2008). Therefore, mTORC1 is thought to be an integral node in a network that couples cellular energy production to consumption.

In this study, we demonstrate that mTORC1 stimulates mitochondrial biogenesis and activity, thereby bolstering ATP production capacity. mTOR inhibitors caused a decrease in ATP levels associated with impaired mitochondrial function and glycolysis. At the molecular level, this is explained by preferential inhibition of translation of a subset of cellular mRNAs that encode for essential nucleus-encoded mitochondrial proteins including the components of complex V and TFAM (transcription factor a, mitochondrial). Moreover, we show that 4E-BPs mediate the stimulatory effect of mTORC1 on the translation of mitochondria-related mRNAs, mitochondrial respiration and biogenesis, and ATP production in vitro and in vivo. These data reveal a feed-forward mechanism by which translation impacts mitochondrial function to maintain energy homeostasis in the cell.

RESULTS

mTOR Regulates Translation of a Subset of Mitochondria-Related mRNAs

We recently identified mRNAs whose translation was affected by mTOR inhibitors (Larsson et al., 2012) using genome-wide polysome profiling (Larsson et al., 2010, 2011). Among the mRNAs whose translation was suppressed after 12 hr treatment with the active-site mTOR inhibitor (asTORi) PP242, those encoding mitochondria-related proteins were highly abundant (14% of target mRNAs) (Table S1). Indeed, pathway analysis using the generally applicable gene-set enrichment (GAGE) method (Luo et al., 2009) revealed a significant enrichment of genes annotated to mitochondria-related functions as translationally suppressed by PP242 (Figure 1A). mRNAs encoding components of complex V (ATP synthase) in the oxidative phosphorylation pathway were the most significantly enriched (Figure 1A) and included ATP synthase subunit delta (ATP5D), ATP5G1, ATP5L, and ATP5O (Figure 1B) (Hoffmann et al., 2010). mRNAs encoding TFAM (transcription factor A, mitochondrial), which promotes mitochondrial DNA replication and transcription (Bonawitz et al., 2006), mitochondrial ribosomal proteins, and NADH dehydrogenase 1 alpha subcomplex assembly factors 2 and 4 (NDUFAF2 and 4), were also significantly enriched (Figures 1A and 1B).

mTOR also regulates transcription of mitochondrial genes via PGC-1α (Blättler et al., 2012; Cunningham et al., 2007). Potential effects of mTOR inhibition on mitochondrial function that are caused by transcriptional mechanisms could therefore obscure those that occur at the level of translation. To exclude this possibility, we compared the effects of PP242 on transcriptional and translational activity, which revealed that after 12 hr treatment PP242 strongly inhibited translation of a subset of mitochondria-related mRNAs, while having only a marginal effect on transcription of the corresponding genes (Figure 1C). Consistently, the assessment of mitochondrial functions upon ectopic expression of the transcriptional coactivators (e.g., PGC-1α) has typically been performed after 48 hr or longer (Lehman et al., 2000; St-Pierre et al., 2003). Thus, 12 hr asTORi treatment is adequate to determine the effects of translation on mitochondrial activity, without substantial interference from transcriptional mechanisms.

We next validated the effect of two asTORi: Ink1341 (derived from the PP242 chemical scaffold [Alain et al., 2012]) and Torin1 (Thoreen et al., 2009) on the translation of several mitochondria-related mRNAs in MCF7 cells using polysome profiling. As reported previously (Thoreen et al., 2009; Yu et al., 2009), the phosphorylation of 4E-BP1, 4E-BP2, and ribosomal protein S6 was abolished by asTORi (Figure 2A). Accordingly, asTORi strongly impaired the eIF4F complex assembly as monitored by a cap pull-down assay (Figure 2B). To directly investigate whether asTORi suppress translation of mitochondria-related mRNAs, polysomes from MCF7 cells treated with asTORi were sedimented in sucrose density gradients to separate efficiently translated mRNAs (associated with heavy polysomes) from those that are poorly translated (associated with light polysomes) (Figure 2C). asTORi inhibited protein synthesis, as illustrated by the decrease in polysome content with a concomitant increase in the 80S peak (Figure 2C). Consistent with previous findings (Alain et al., 2012; Hsieh et al., 2012; Thoreen et al., 2012), Ink1341 and Torin1 did not induce complete disassembly of polysomes (Figure 2C), indicating that these compounds selectively block translation of a subset of mRNAs. Indeed, 12 hr Torin1 treatment caused a ~35% decrease in global translation relative to a control as measured by [^{35}S]methionine/cysteine labeling (Figure S1). Thus, we assessed the effects of Ink1341 and Torin1 on polysomal distribution of ATP5O, ATP5D, and TFAM mRNAs, which were identified as mTOR-sensitive (Figure 1B), and β-actin mRNA, which is resistant to mTOR inhibitors (Hsieh et al., 2012; Larsson et al., 2012). asTORi suppressed translation of ATP5D, ATP5O, and TFAM mRNAs, as illustrated by a shift of these mRNAs toward lighter polysomes (Figure 2D), whereas asTORi failed to shift the β-actin mRNA (Figure 2D). Consistently, ATP5O, ATP5D, and TFAM but not β-actin protein levels were decreased in asTORi-treated cells (Figure 2A). In contrast to ATP5O, ATP5D, and TFAM, expression of COX4I1 protein that is a component of oxidative phosphorylation complex IV (Fornuskova et al., 2010) was not sensitive to asTORi (Figure 2A). These data indicate that mTOR controls translation of a subset of, but not all, mitochondria-related mRNAs.

mTOR Controls Mitochondrial Function and ATP Production

Since asTORi inhibited translation of ATP5D, ATP5O, and TFAM mRNAs, we wished to investigate the effects of asTORi on mitochondrial activity. MCF7 cells were treated with a vehicle, PP242 or Ink1341, for 12 hr, and the rate of mitochondrial respiration was determined using a Clark-type electrode (Figures 3A–3D). asTORi decreased total mitochondrial respiration (~35%) as compared to vehicle control (Figure 3A). There are two types of mitochondrial respiration: coupled respiration (drives oxidative phosphorylation and ATP synthesis) and uncoupled respiration (represents proton leak reactions) (Rolfe and Brown, 1997). asTORi decreased both coupled (~30%) and uncoupled respiration (~40%) (Figures 3B and 3C). The fraction of cellular respiration dedicated to coupling and uncoupling remained constant between asTORi- and vehicle-treated cells (Figure 3D). Similar

A

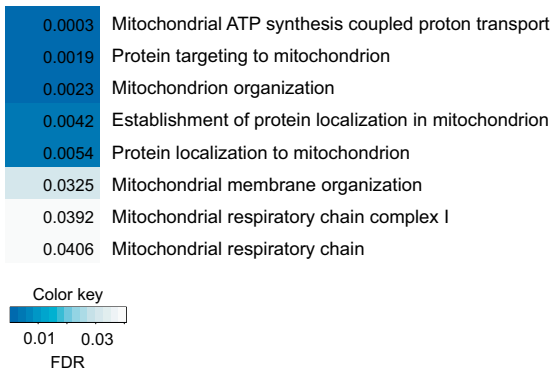

B

Gene Symbol	Gene ID	Gene Description	% decrease of translational activity by PP242 (FDR < 0.05)
Oxidative phosphorylation Complex V			
ATP5D	513	ATP synthase, H+ transporting, mitochondrial F1 complex, delta subunit	34
ATP5G1	516	ATP synthase, H+ transporting, mitochondrial Fo complex, subunit C1	58
ATP5L	10632	ATP synthase, H+ transporting, mitochondrial Fo complex, subunit G	36
ATP5O	539	ATP synthase, H+ transporting, mitochondrial F1 complex, O subunit	41
Oxidative phosphorylation Complex I			
NDUFAF2	91942	NADH dehydrogenase (ubiquinone) 1 alpha subcomplex, assembly factor 2	45
NDUFAF4	29078	NADH dehydrogenase (ubiquinone) 1 alpha subcomplex, assembly factor 4	37
NDUFS6	4726	NADH dehydrogenase (ubiquinone) Fe-S protein 6	60
Transcription factor			
TFAM	7019	transcription factor A, mitochondrial	35
Mitochondrial ribosomal proteins			
MRPL12	6182	mitochondrial ribosomal protein L12	39
MRPL23	6150	mitochondrial ribosomal protein L23	41
MRPL27	51264	mitochondrial ribosomal protein L27	42
MRPL30	51263	mitochondrial ribosomal protein L30	35
MRPL36	64979	mitochondrial ribosomal protein L36	33
MRPL47	57129	mitochondrial ribosomal protein L47	43
MRPL48	51642	mitochondrial ribosomal protein L48	42
MRPS6	64968	mitochondrial ribosomal protein S6	49
MRPS12	6183	mitochondrial ribosomal protein S12	49
MRPS34	65993	mitochondrial ribosomal protein S34	35

C

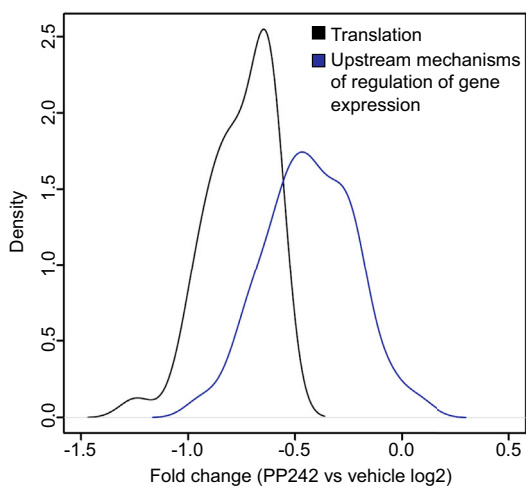

Figure 1. Genome-wide Analysis Indicates that Translation of a Subset of mRNAs Encoding Mitochondria-Related Proteins Is Selectively Suppressed by asTORi

(A) Cellular processes regulated by genes that are translationally suppressed by asTORi PP242 were determined by GAGE analysis. Significantly enriched mitochondrial related functions were selected and are shown together with their associated enrichment false discovery rates (FDR).

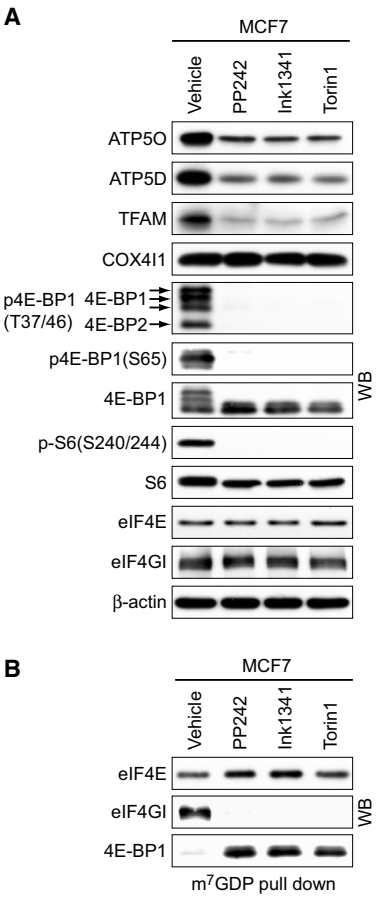

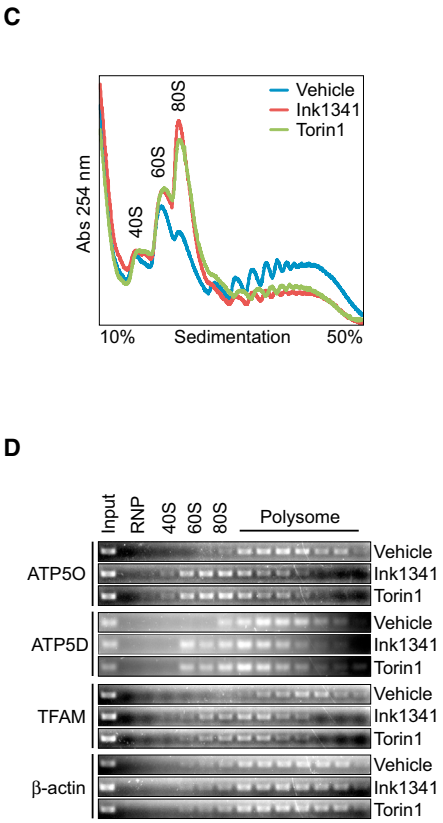

Figure 2. Translation Regulation of Mitochondrial Proteins by mTOR

(A) Levels of proteins in cells treated with the indicated compounds for 12 hr were determined by western blotting. eIF4E and β-actin were used as loading controls.

(B) m^7GTP pull-down assay of proteins from extracts in (A).

(C) Polysome profiles of cells treated with vehicle, Ink1341, or Torin1 for 12 hr. Absorbance at 254 nm was recorded continuously. 40S, 60S, and 80S denote the positions of corresponding ribosomal subunits and monosomes.

(D) Distribution of ATP5O, ATP5D, TFAM, and β-actin mRNAs across the density gradients from (C) was determined by RT-sqPCR. See also Figure S1.

findings were obtained in mouse embryonic fibroblasts (MEFs) (Figures S2A–S2D), thus indicating that the effects of asTORi on respiration are not limited to malignant cells. Therefore, asTORi exert a general effect on cellular energy production by suppressing respiration in proliferating cells.

Since our data showed that asTORi inhibited mRNA translation and mitochondrial respiration, we asked whether asTORi also change the steady-state levels of metabolites involved in major bioenergetic pathways. Intracellular metabolite levels in MCF7 cells were measured using gas chromatography-mass spectrometry (GC-MS) and ^{1}H nuclear magnetic resonance (NMR) spectroscopy. Ink1341 and PP242 strongly reduced tricarboxylic acid (TCA) cycle intermediates as compared to control (Figures 3E and S2E). This striking decrease in TCA cycle intermediates, in conjunction with diminished respiration, indicates reduced mitochondrial functions. asTORi also induced intracellular accumulation of glucose (58%) and decreased lactate and pyruvate (51% and 45%, respectively; Figures S2F and S2G), which is consistent with the stimulatory role of mTOR in glycolysis (Düvel et al., 2010; Hagiwara et al., 2012; Yuan et al., 2012). To investigate the effects of asTORi on carbon flux through glycolysis and the TCA cycle, we cultured cells in a medium containing the uniformly labeled D[U-^{13}C]glucose for 30 min and measured ^{13}C enrichment of intracellular metabolites by GC-MS (Figures 3F, S2H, and S2I) (Nanchen et al., 2007). In the cytosol, D[U-^{13}C] glucose through glycolysis produces pyruvate m+3 (pyruvate mass shift by three units from ^{13}C), which is translocated to the mitochondria or metabolized to lactate m+3 (Figure S2H). In the mitochondria, pyruvate m+3 is converted to acetyl-CoA (coenzyme A) m+2, which enters the TCA cycle to produce citrate m+2 upon reaction with oxaloacetate (Figure S2H). Processing of citrate m+2 in the second round of the TCA cycle produces citrate m+4 (Figure S2H). In vehicle-treated cells, most citrate molecules contained glucose-derived ^{13}C (Figure 3F, upper). In Ink1341-treated cells, the proportion of citrate m+4 was dramatically decreased, and the one citrate m+2 was also decreased, while the one unlabeled citrate (m+0) was increased (Figure 3F, upper). The proportion of isocitrate m+2 and m+4 as well as α-ketoglutarate m+2 and m+4 were also diminished in Ink1341-treated cells (Figure 3F, lower). Furthermore, Ink1341 increased the proportion of unlabeled pyruvate and lactate (m+0) (Figure S2I). These data show that mTOR activity regulates the flux of glucose through TCA cycle and glycolysis. In addition, asTORi treatment decreased mitochondrial DNA content and mitochondrial mass (Figures 3G–3I). Finally, cellular ATP

(B) A subset of mRNAs encoding mitochondrial proteins that are translationally suppressed following 12 hr treatment with PP242 (FDR < 0.05; percentage decrease relative to control is indicated).

(C) Kernel density plot shows a comparison of fold changes (PP242 versus vehicle treatment) in the upstream mechanisms of regulation of gene expression (e.g., transcription) that are reflected in steady-state mRNA levels (blue line) or translation (black line) for the subset of genes described in Table S1. Stronger shift of "translation" curve toward ordinate compared to that observed for steady-state mRNA levels indicates that after 12 hr of PP242 treatment, downregulation of genes described in Table S1 occurs mostly at the translational level, whereas the contribution of the upstream mechanisms of regulation of gene expression (e.g., transcription) is minimal. See also Table S1.

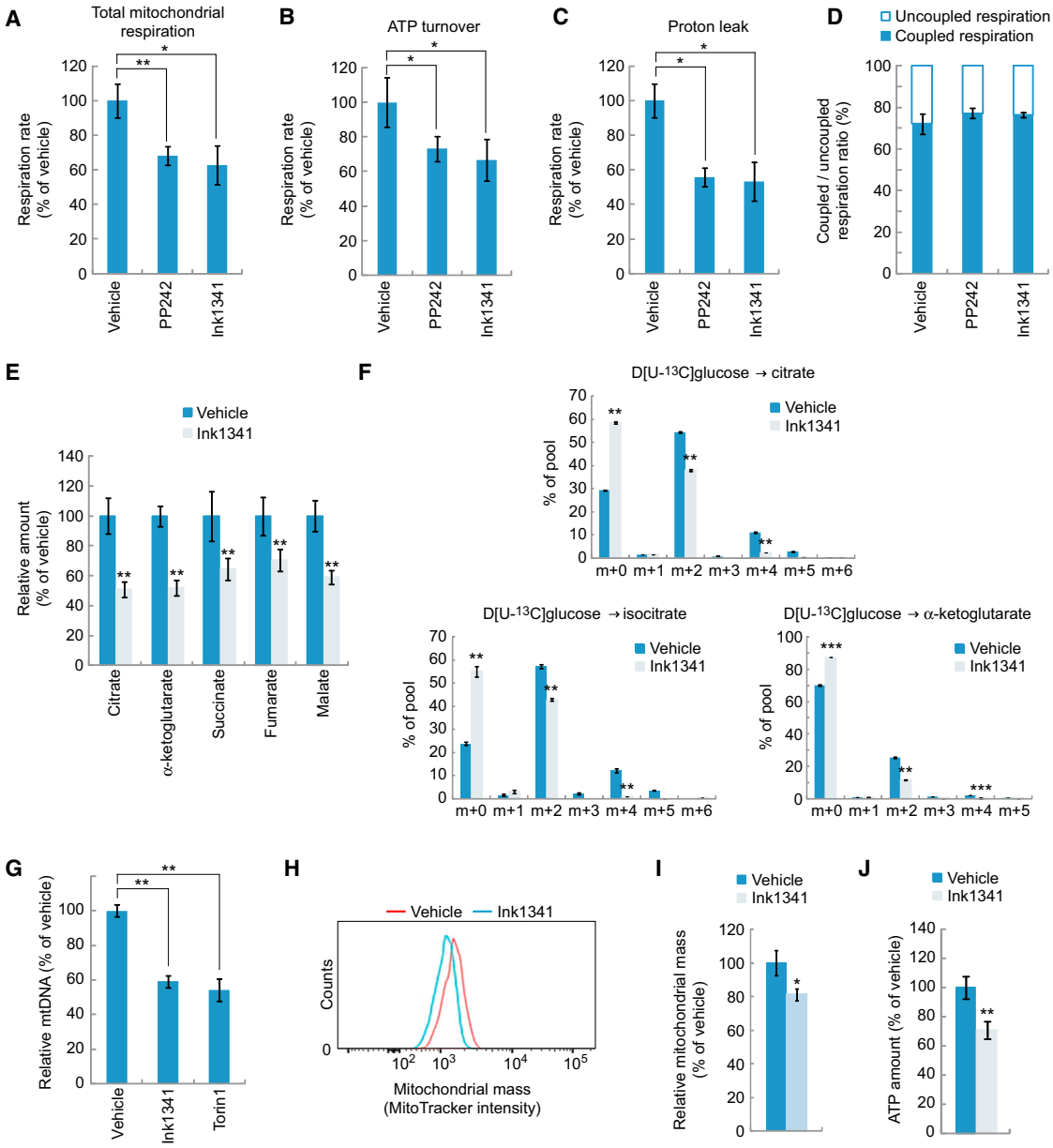

Figure 3. asTORi Suppress Mitochondrial Functions and ATP Production

(A–D) Total mitochondrial respiration (A), ATP turnover (B), proton leak (C), and coupled/uncoupled respiration ratio (D) in cells treated with vehicle, PP242, or Ink1341 for 12 hr were measured using a Clark-type electrode. ATP turnover and proton leak represent oligomycin-sensitive and -insensitive respiration, respectively.

(E) Quantification of levels of TCA cycle intermediates (citrate, α-ketoglutarate, succinate, fumarate, and malate) from cells treated with vehicle or Ink1341. Metabolites were extracted, profiled by GC-MS, and normalized to cell number.

(F) Mass isotopomer distribution analysis of citrate, isocitrate, and α-ketoglutarate in cells described in (E). Cells were incubated with D[U-^{13}C]glucose, and isotopomers with the indicated mass shift were analyzed.

(G) Relative mitochondrial DNA content from cells treated with vehicle, Ink1341, or Torin1 for 24 hr was determined by qPCR. Mitochondrial DNA content was normalized to genomic DNA content.

(H and I) Mitochondrial mass in cells described in (G) was estimated by monitoring mean fluorescence intensity of MitoTracker by flow cytometry.

(J) Quantification of cellular levels of ATP in cells described in (E). Metabolites were extracted, profiled by LC-MS, and normalized to cell number. Data represent mean ± SD of three independent experiments, except for (E) and (F), where a representative experiment of three independent experiments (each carried out in triplicate) is presented. *$p < 0.05$. **$p < 0.01$. See also Figure S2.

concentration was measured by liquid chromatography-mass spectrometry (LC-MS). Consistent with the downregulation of mitochondrial functions and glycolysis, a significant decrease (~30%) in the ATP pool was observed in asTORi-treated cells as compared to control (Figure 3J). These findings imply that the inhibition of mitochondria-associated mRNA translation by asTORi results in downregulation of TCA cycle activity and ATP production capacity.

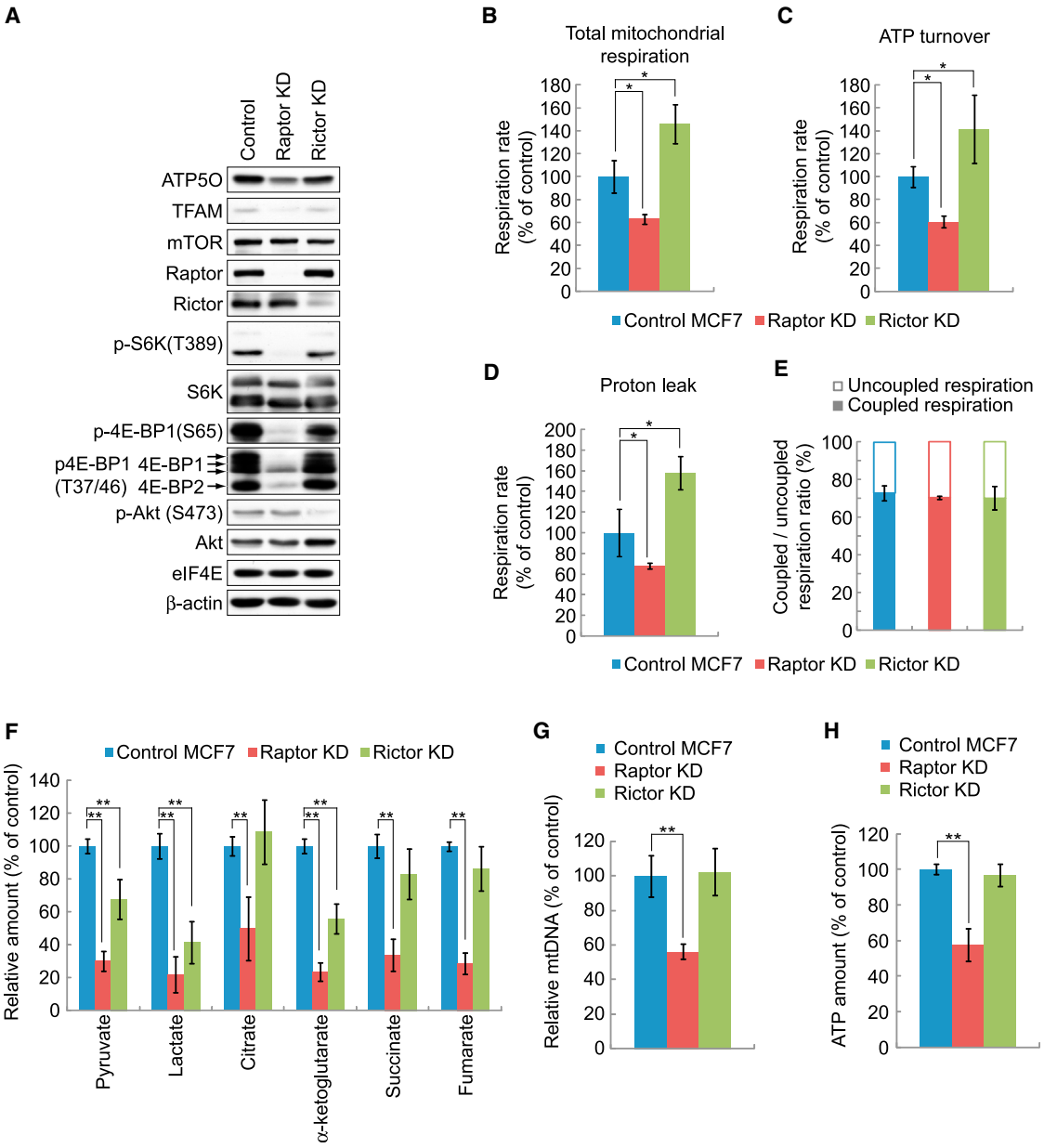

Figure 4. mTORC1-Dependent Regulation of Mitochondrial Function and ATP Production

(A) Levels and phosphorylation status of the indicated proteins in MCF7 cells transduced with control, raptor, or rictor shRNA were determined by western blotting. β-actin and eIF4E were used as loading controls.

(B–E) Total mitochondrial respiration (B), ATP turnover (C), proton leak (D), and coupled/uncoupled respiration rate (E) in cells described in (A) were determined using a Clark-type electrode.

(F) Levels of pyruvate, lactate, and TCA cycle intermediates (citrate, α-ketoglutarate, succinate, and fumarate) from cells in (A). Metabolites were extracted, profiled by GC-MS, and normalized to cell number.

(G) Relative mitochondrial DNA content from cells described in (A) was assessed by qPCR. Mitochondria DNA content was normalized to genomic DNA content.

(H) Quantification of cellular ATP levels from cells described in (A). ATP levels were normalized to cell number. Data represent mean ± SD of three independent experiments. For (F), a representative experiment of three independent experiments (each carried out in triplicate) is presented. *$p < 0.05$. **$p < 0.01$.

mTORC1, but Not mTORC2, Induces Expression of Nucleus-Encoded Mitochondrial Proteins and Mitochondrial Function

To determine which mTOR complex is a major regulator of mitochondrial function, MCF7 cells were depleted of raptor or rictor, which are specific components of mTORC1 and mTORC2, respectively (Figure 4A). Raptor depletion decreased the phosphorylation of S6K, 4E-BP1, and 4E-BP2, while rictor knockdown reduced the phosphorylation of Akt (Figure 4A) (Sarbassov et al., 2005). Depletion of raptor, but not rictor, caused a decrease in ATP5O and TFAM proteins (Figure 4A). Depletion of raptor was paralleled by the reduction in mitochondrial respiration (Figures

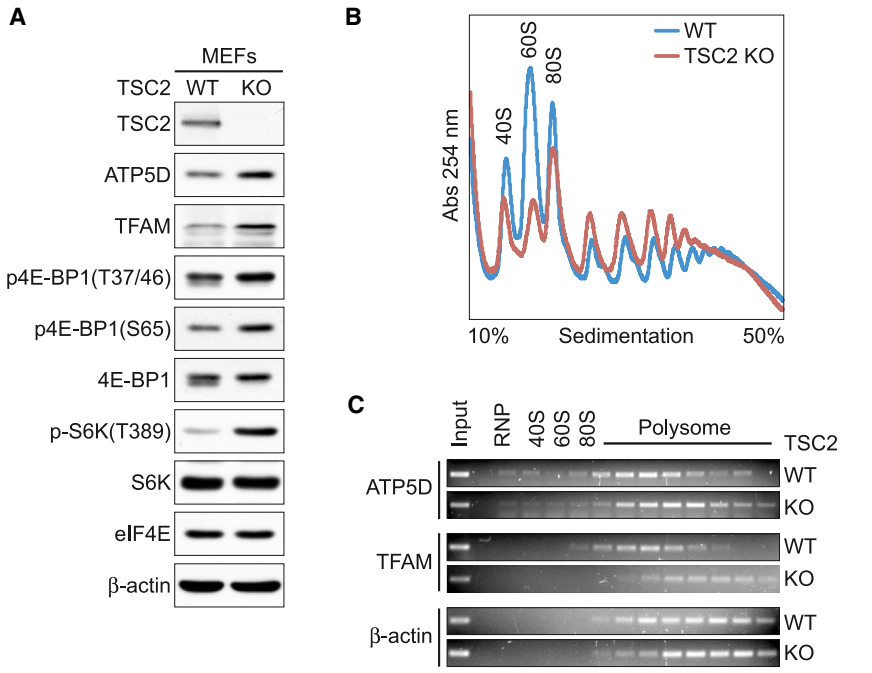

Figure 5. Constitutive mTORC1 Activation Stimulates Mitochondrial Function and ATP Production

(A) Levels and phosphorylation status of the indicated proteins in WT and TSC2 KO MEFs were determined by western blotting. β-actin was used as a loading control.

(B) Polysome profiles of cells described in (A). Absorbance at 254 nm was continuously recorded. 40S, 60S, and 80S denote the corresponding ribosomal subunits and monosomes, respectively.

(C) Polysome distribution of ATP5D, TFAM, and β-actin mRNAs in cells described in (A) was determined by RT-sqPCR.

(D) Total mitochondrial respiration, ATP turnover, and coupled/uncoupled respiration ratio of cells described in (A) were measured using a Clark-type electrode.

(E) Relative mitochondrial DNA content from cells described in (A) was determined by qPCR. Mitochondria DNA content was normalized to genomic DNA content.

(F) Quantification of cellular ATP levels from cells described in (A). ATP levels were normalized to cell number. Data represent mean ± SD of three independent experiments. *$p < 0.05$. **$p < 0.01$.

4B–4E) and the amounts of TCA cycle intermediates pyruvate and lactate (Figure 4F). This indicates that mTORC1 bolsters mitochondrial function, TCA cycle, and glycolysis. In turn, knockdown of rictor resulted in a decrease in the amounts of pyruvate and lactate and stimulation of mitochondrial respiration (Figures 4B–4F), which is consistent with recent reports (Betz et al., 2013; Hagiwara et al., 2012; Schieke et al., 2006; Yuan et al., 2012). Interestingly, depletion of rictor also decreased the amount of α-ketoglutarate (Figure 4F). In MCF7 cells, the majority of α-ketoglutarate (~70%) was unlabelled (Figure 3F). This suggests that in MCF7 cells, α-ketoglutarate is derived from other metabolic pathways such as glutaminolysis (Ward and Thompson, 2012), thereby suggesting that mTORC2 may regulate this process. In addition, raptor knockdown diminished intracellular ATP levels and mtDNA content relative to control, whereas depletion of rictor had no effect (Figures 4G and 4H). These findings indicate that the effects of mTOR signaling on mitochondrial biogenesis and functions are mostly mediated by mTORC1.

Ras-homolog enriched in brain (Rheb) is a small GTPase that activates mTORC1 (Inoki et al., 2003; Tee et al., 2003). Tuberous sclerosis complex (TSC1/2) acts as a GAP toward Rheb, thereby suppressing mTORC1 signaling (Laplante and Sabatini, 2012). We used TSC2 knockout (KO) MEFs (Zhang et al., 2003) to determine the effects of mTORC1 hyperactivation on mitochondrial biogenesis and functions. As expected, TSC2 KO MEFs exhibited elevated phosphorylation of 4E-BP1 and S6K1 as compared to wild-type (WT) cells (Figure 5A). Moreover, levels of ATP5D and TFAM proteins were also higher in TSC2 KO than in WT MEFs (Figure 5A).

As reported previously, the proportion of ribosomes engaged in polysomes was higher in TSC2 KO as compared to WT MEFs (Figure 5B) (Conn and Qian, 2013; Sun et al., 2011). Importantly, ATP5D and TFAM but not β-actin mRNAs were shifted toward heavy polysome fractions in TSC2 KO as compared to WT MEFs, indicating that loss of TSC2 selectively bolsters translation of ATP5D and TFAM mRNAs (Figure 5C). Consistent with previous findings (Cunningham et al., 2007; Schieke et al., 2006), loss of TSC2 expression increased mitochondrial respiration, mitochondrial DNA content, and ATP levels (Figures 5D–5F). These results further support the conclusion that mTORC1 modulates mitochondrial activity and biogenesis by stimulating translation of a subset of mitochondria-related mRNAs.

4E-BPs Are Mediators of mTORC1-Dependent Control of Mitochondrial Function

4E-BPs are implicated in the regulation of mitochondrial function in *Drosophila* and mammals (Goo et al., 2012; Zid et al., 2009). Therefore, we investigated the role of 4E-BPs in mediating the effects of asTORi on translation of mitochondria-related mRNAs. To this end, we depleted 4E-BP1 and 4E-BP2 (4E-BP1/2) from MCF7 cells. asTORi impaired global mRNA translation to a higher extent in control versus 4E-BP1/2-depleted cells, as illustrated by a stronger increase in the 80S monosome peak and a decrease in polysomes (Figure 6A). Whereas 4E-BP1/2 depletion did not affect polysome distribution of β-actin mRNA (Figure 6B, upper), it prevented the Ink1341-induced shift of TFAM and ATP5O mRNAs toward lighter polysomes (Figure 6B, lower). Therefore, 4E-BPs act as major mediators of mTORC1 on translation of TFAM and ATP5O mRNAs. Accordingly, asTORi decreased ATP5O and TFAM protein levels in control, but not in 4E-BP1/2-depleted cells (Figure 6C).

We next studied the effects of 4E-BPs on mitochondrial respiration. Although depletion of 4E-BPs did not affect mitochondrial respiration in untreated MCF7 cells (Figure S3A), it significantly relieved asTORi-induced inhibition of this process as compared to a control (Figure 6D). Parallel results were obtained with 4E-BP1 and 4E-BP2 double knockout (4E-BP DKO) MEFs (Figures S3B and S3C). To investigate the impact of 4E-BP1/2 depletion on mTORC1-dependent regulation of TCA cycle, we performed glucose flux analyses (Figures 6E and S3D). In control cells, Ink1341 diminished the proportion of ^{13}C-labeled TCA cycle intermediates, which was accompanied by an increment of unlabeled metabolites (Figure 6E). In contrast, carbon flux of TCA cycle intermediates in 4E-BP1/2-depleted cells was partially resistant to Ink1341 as compared to control cells (Figure 6E). Ink1341 also reduced carbon flux from glucose to pyruvate and lactate in control cells, but less so in 4E-BP1/2-depleted cells (Figure S3D). Finally, depletion of 4E-BPs mitigated the effects of asTORi on mitochondrial DNA content, mitochondrial mass, and intracellular ATP levels (Figures 6F–6H). These findings show that the inhibition of mitochondrial activity and biogenesis by asTORi is predominantly mediated by 4E-BPs.

S6Ks, PGC-1α, and HIF-1α Are Not Major Mediators of the Effects of Short-Term mTOR Inhibition on Mitochondria

In addition to 4E-BPs, S6Ks also mediate the effects of mTORC1 on translation (Roux and Topisirovic, 2012). Using S6K1/2 double knockout (S6K DKO) MEFs and S6K DKO MEFs in which expression of S6K1 and 2 was reconstituted (Figure S4A) (Dowling et al., 2010), we show that neither under basal conditions nor in response to asTORi treatment do S6Ks affect mitochondrial respiration and glucose flux to pyruvate and lactate (Figures S4B–S4E). However, loss of S6K expression resulted in decreased glucose flux to citrate under basal conditions (Figure S4F) and attenuated inhibitory effects of asTORi on citrate production (Figure S4H). Citrate metabolism plays a key role in fatty acid synthesis, and it has been reported that S6Ks are major mediators of mTOR function in lipogenesis (Düvel et al., 2010). Therefore, it is likely that S6Ks modulate citrate production downstream of mTORC1 in conjunction with their role in lipid synthesis. Nonetheless, these results demonstrate that S6Ks are not major mediators of mTORC1 function in mitochondrial biogenesis and activity.

Although PGC-1α deficiency (Figure S5A) impaired mitochondrial respiration (Figure S5B), asTORi inhibited this process to a similar extent in WT and PGC-1α KO MEFs (Figure S5C). HIF-1α deficiency did not affect basal mitochondrial respiration (Figure S5E) or influence the effects of asTORi on mitochondrial respiration and glucose flux (Figures S5F and S5G). Therefore, PGC-1α and HIF-1α do not appear to be required for the suppression of mitochondrial function that is observed after 12 hr of mTOR inhibition.

4E-BPs and Autophagy Independently Mediate the Effects of asTORi on Mitochondria

mTORC1 inhibition activates autophagy, which is a major pathway of degradation of mitochondria (Fleming et al., 2011). To investigate the possible role of autophagy in mediating the effects of asTORi treatment on mitochondria, we generated WT and 4E-BP DKO MEFs in which autophagy was impaired by ATG5 depletion (Figure S6A). As expected, asTORi induced autophagy in control cells as illustrated by a reduction in LC3A-I and concomitant increase in LC3A-II, but not in ATG5-depleted cells (Figure S6A). ATG5 reduction partially relieved the effects of asTORi on mitochondrial DNA content and mass in WT MEFs (Figures S6B–S6D). Strikingly, ATG5 depletion in 4E-BP DKO MEFs rescued the reduction caused by asTORi on mitochondrial DNA content and mass (Figures S6B–S6D). These findings indicate that translational regulation through 4E-BPs and autophagy collaboratively mediate the effects of mTORC1 on mitochondria.

Re-expression of TFAM Attenuates the Effects of asTORi on Mitochondrial DNA Synthesis

TFAM promotes mitochondrial biogenesis by stimulating mitochondrial DNA replication and transcription (Bonawitz et al., 2006). To determine whether suppression of TFAM translation underlies the effects of the mTORC1/4E-BP pathway on mitochondrial biogenesis, we used a TFAM cDNA lacking its 5′ UTR whose expression is resistant to asTORi treatment (Figure S7A). Consistent with previous findings (Bonawitz et al., 2006), TFAM overexpression increased basal mitochondrial DNA content (Figure S7B). More importantly, TFAM overexpression attenuated the effects of Ink1341 on mitochondrial DNA content (Figure S7C). These data indicate that suppression of TFAM expression at the level of translation plays a major role

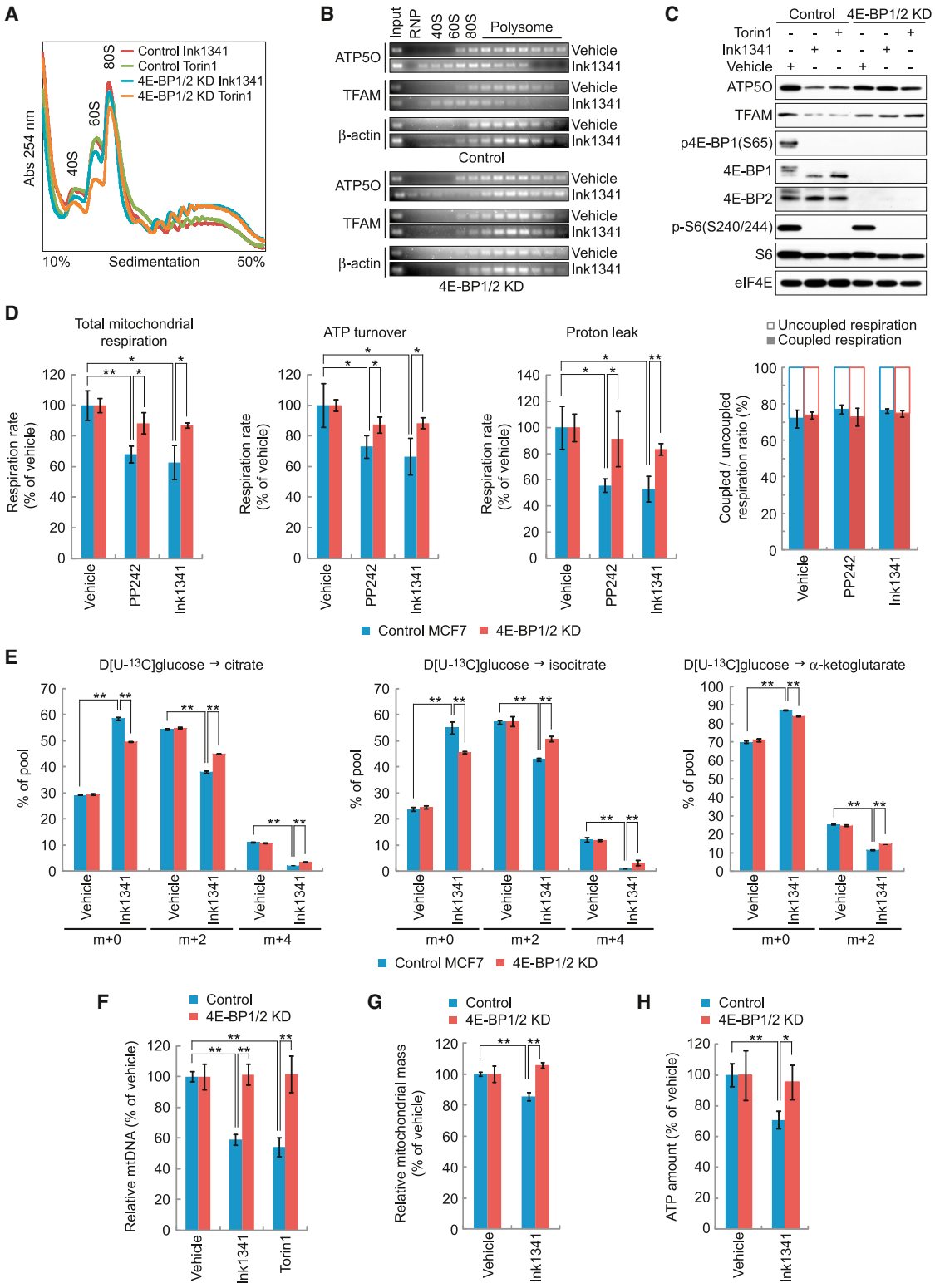

Figure 6. 4E-BPs Are Required for mTOR-Dependent Mitochondrial Function and Translation of mRNAs Encoding Mitochondrial Proteins

(A) Polysome profiles of MCF7 cells transduced with a control or 4E-BP1/2 shRNA and treated with Ink1341 or Torin1 for 12 hr. Absorbance at 254 nm was continuously recorded. 40S, 60S, and 80S denote the corresponding ribosomal subunits and monosomes, respectively.

(B) Polysome distribution of ATP5O, TFAM, and β-actin mRNAs in cells described in (A) was determined by RT-sqPCR.

(C) Levels and phosphorylation status of the indicated proteins in cells described in (A) and treated with asTORi were determined by western blotting.

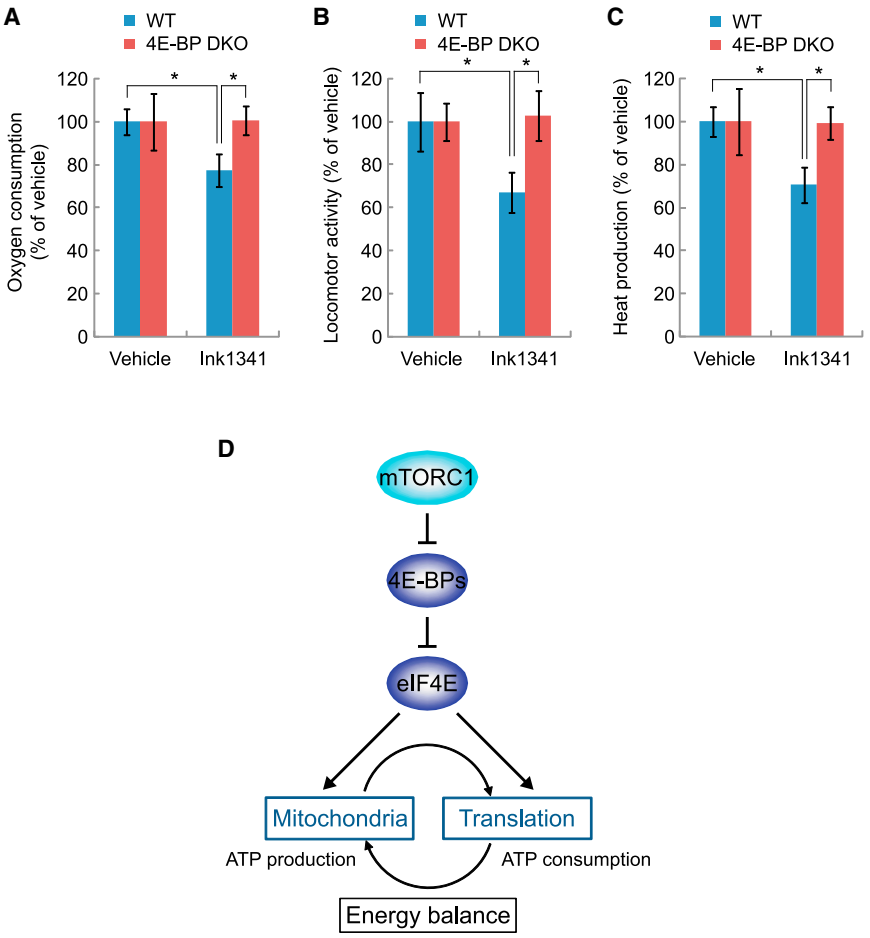

Figure 7. The 4E-BP-Dependent Effect of asTORi on Respiration In Vivo and Proposed Model of Cross-Regulation of mRNA Translation and Energy Metabolism

(A) Oxygen consumption of WT and 4E-BP DKO mice with intraperitoneal administration of vehicle or Ink1341 (3 mg/kg body weight). Oxygen consumption was measured over 24 hr, and average oxygen consumption per hour during dark phase was normalized to body mass (see Experimental Procedures).

(B) Locomotor activity measured by photobeam breaks.

(C) Heat production calculated with a calorific value based on the observed respiratory exchange ratio and the measured oxygen consumption. Data represent mean ± SD. n = 5 per group. *p < 0.05. **p < 0.01.

(D) Model of translational control of mitochondrial function: mTORC1 prevents 4E-BPs from binding to eIF4E and promotes translation of mRNAs encoding mitochondria-related proteins, thereby bolstering mitochondrial energy production. This increase in mitochondrial ATP production fuels mRNA translation, which is one of the most energy consuming processes in the cell. Energy balance between consumption and production is therefore maintained via the mTORC1/4E-BP pathway.

in mTORC1/4E-BP-dependent regulation of mitochondrial DNA synthesis.

mTORC1 Controls Mitochondrial Respiration through 4E-BP Inhibition In Vivo

mTORC1 signaling controls oxygen consumption in mice (Polak et al., 2008; She et al., 2007). To investigate the effects of asTORi on in vivo respiration, WT and 4E-BP DKO mice were treated daily with Ink1341 for 2 weeks. Ink1341 inhibited 23% oxygen consumption in WT, but not in 4E-BP DKO mice (Figure 7A). Consistent with a recent finding that a tissue-specific raptor knockout mouse exhibits decreased locomotor activity (Bentzinger et al., 2008; Polak et al., 2008), Ink1341 suppressed locomotor activity in WT mice, whereas this effect was absent in 4E-BP DKO mice (Figure 7B). Also, Ink1341 suppressed heat production in WT, but not in 4E-BP DKO mice (Figure 7C). Thus, consistent with the in vitro findings, mTORC1 controls mitochondrial respiration and energy metabolism through 4E-BPs in vivo.

DISCUSSION

In this study we describe a feed-forward mechanism whereby translation of nucleus-encoded mitochondria-related mRNAs is modulated via the mTORC1/4E-BP pathway to induce mitochondrial ATP production capacity and thus provide sufficient energy for protein synthesis (Figure 7D).

Hyperactivation of mTOR signaling is frequently observed in cancer (Laplante and Sabatini, 2012), and eIF4E overexpression is tumorigenic in vitro and in vivo (Avdulov et al., 2004; Lazaris-Karatzas et al., 1990; Ruggero et al., 2004; Wendel et al.,

(D) Total mitochondrial respiration, ATP turnover, proton leak, and coupled/uncoupled respiration rate of cells described in (A) and treated with asTORi for 12 hr were determined using a Clark-type electrode.

(E) Mass isotopomers distribution analysis of citrate, isocitrate, and α-ketoglutarate in cells described in (A) and treated with asTORi for 12 hr. Cells were incubated with D[U-^{13}C]glucose, and isotopomers with the indicated mass shift were analyzed by GC-MS.

(F) Relative mitochondrial DNA content from cells described in (A) and treated with asTORi for 24 hr was determined by qPCR. Mitochondrial DNA content was normalized to genomic DNA content.

(G) Mitochondrial mass in cells described in (A) treated with asTORi for 24 hr was estimated by monitoring mean fluorescence intensity of MitoTracker by flow cytometry.

(H) Quantification of cellular ATP levels in the cells described in (E). Data represent mean ± SD of three independent experiments. For (E), a representative experiment of three independent experiments (each carried out in triplicate) is presented. *p < 0.05. **p < 0.01. See also Figures S3, S4, S5, S6, and S7.

2004). Although altered glucose metabolism (i.e., Warburg effect) is a hallmark of cancer cells (Vander Heiden et al., 2009), these cells also rely on mitochondrial intermediates to generate building blocks (e.g., nucleic acids and phospholipids) necessary for neoplastic growth (Ward and Thompson, 2012). The mTORC1/4E-BP pathway promotes ATP production capacity by mitochondria, as well as cell cycle progression (Dowling et al., 2010). Thus, mTORC1 drives cell proliferation and neoplastic growth by simultaneously activating translation of mRNAs that encode proteins involved in cellular energy production and cell cycle progression.

Notably, in spite of the reduced ATP utilization caused by the inhibition of protein synthesis, an increase in cellular ATP concentration was not observed after mTOR inhibition (Figure 3J), which can be explained by the concomitant reduction in mitochondrial respiration (Figure 3B). Indeed, asTORi-induced impairment in ATP production is accompanied by reduction in ATP consumption, which results in a state of metabolic quiescence. These data suggest that asTORi may induce a state of "metabolic dormancy" in cancer cells, which would predict a cytostatic rather than cytotoxic effect of asTORi in the clinic (Benjamin et al., 2011).

mTOR is a multifaceted kinase that employs a number of effectors to exert its biological functions (Laplante and Sabatini, 2012). Accordingly, 4E-BPs affect TCA cycle in conjunction with other mTORC1 targets (e.g., S6Ks; Figures S4F and S4H) and mTORC2 (Figure 4F) that have been previously reported to modulate lipogenesis and glycolysis (Düvel et al., 2010; Hagiwara et al., 2012; Yuan et al., 2012). However, our results demonstrate that 4E-BPs act as major mediators of the effects of mTORC1 on mitochondrial biogenesis and function. In addition to stimulation of mitochondrial biogenesis by antagonizing 4E-BP-dependent translational repression of mitochondria related mRNAs, mTORC1 inhibits mitochondrial degradation by suppressing autophagy (Figures S6B–S6D). These findings suggest coordination of translational and autophagy programs that underpin important biological effects of mTORC1 signaling.

mTORC1 also stimulates mitochondrial respiration and biogenesis via the transcriptional regulators PGC-1α and HIF-1α (Cunningham et al., 2007; Düvel et al., 2010). However, neither PGC-1α nor HIF-1α appeared to impair mitochondrial activity after 12 hr inhibition of mTOR (Figure S5). Accordingly, we did not observe major changes in mRNA steady-state levels of a subset of mitochondria-related genes as a consequence of mTOR inhibition (Figure 1C). It is well established that the changes in gene expression that occur at the level of transcription are heralded by those that take place at the posttranscriptional level (Anderson, 2010). Therefore, it is likely that mTORC1-dependent changes in translation of mitochondria-related mRNAs precede transcriptional regulation. PGC-1α-dependent transcriptional change of mitochondria-related genes was observed in myoblasts in which mTORC1 was inhibited for at least 16 hr (Blättler et al., 2012). Moreover, mitochondria-related genes whose expression is regulated by mTORC1 at the level of translation (ATP5O and ATP5D) were not identified as transcriptional targets of mTORC1 (Cunningham et al., 2007). Hence, it is conceivable that mTOR drives mitochondrial function by simultaneously orchestrating translational and transcriptional programs to modulate expression of mitochondria-related genes.

Two recent studies suggested that the inhibition of mTORC1 by asTORi suppresses 5′ TOP mRNA translation in a 4E-BP-dependent manner (Hsieh et al., 2012; Thoreen et al., 2012). Herein, using a battery of well-established biochemical and functional assays, we demonstrate that the mTORC1/4E-BP pathway stimulates mitochondrial functions by enhancing the translation of a subset of mitochondria-related mRNAs, which largely do not harbor 5′ TOP elements.

In summary, we demonstrate that the mTORC1/4E-BP pathway controls cellular energy homeostasis via translation of nucleus-encoded mitochondria-related genes. This uncovers an important mechanism that explains the role of mTOR signaling in diseases characterized by metabolic perturbations, such as cancer.

EXPERIMENTAL PROCEDURES

Genome-wide Analysis of mRNA Translation Following Treatment with PP242

We used data sets containing steady-state and polysome-associated mRNA obtained from MCF7 cells treated with vehicle or PP242 for 12 hr from our previous study that were deposited at the Gene Expression Omnibus (GEO, GSE36847) (Larsson et al., 2012). Differential translation was calculated using anota analysis (Larsson et al., 2010, 2011), which corrects changes in polysome-associated mRNA for changes in cytoplasmic steady-state mRNA. We used GAGE (Luo et al., 2009) to identify cellular processes (as defined by the Gene Ontology Consortium) showing a significant gene set enrichment among genes that were translationally suppressed (using data from the anota analysis) following treatment with PP242. We applied the "rank.test" option in GAGE using signed (direction of regulation) −log10(FDR) as input data within the "gage" bioconductor package (Gentleman et al., 2004). Cellular processes that showed an enrichment in FDR < 0.05 and were related to mitochondrial function were selected (shown in Figure 1A). We also compared fold changes (PP242 treatment versus control) in steady-state mRNA levels and translation activity (i.e., obtained by anota analysis) for the subset of mitochondrial genes that were identified as differentially regulated at the level of translation following treatment with PP242. Kernel densities for the observed fold changes (PP242 versus vehicle treatment) were obtained using the "density" function in "R" (http://www.r-project.org) with default settings and presented in Figure 1C.

Cell Culture, Lentivirus shRNA Silencing, and mTOR Inhibitors

Cell culture and lentivirus shRNA silencing were carried out as described (Dowling et al., 2010). The information about all MEFs is described in Supplemental Experimental Procedures. For lentivirus production, lentiviral vectors were cotransfected into HEK293T cells with the lentivirus packaging plasmids PLP1, PLP2, and PLP-VSVG (Invitrogen) using Lipofectamine (Invitrogen). Supernatants were collected 48 and 72 hr postinfection, passed through a 0.45 μm nitrocellulose filter, and applied on target cells with polybrene (1 μg/ml). Cells were reinfected the next day and selected with puromycin (5 μg/ml) for 48 hr. The information about lentiviral vectors is described in Supplemental Experimental Procedures. PP242 and Ink1341 were provided by Intellikine, and Torin1 was obtained from Tocris Bioscience. For all experiments, cells were seeded at ~50% confluency, grown overnight, and treated with vehicle (DMSO), PP242 (2.5 μM), Ink1341 (250 nM), or Torin1 (250 nM).

Polysome Profiling, RNA Isolation and RT-sqPCR

Polysome profiling and RT-sqPCR were carried out as described (Dowling et al., 2010). Briefly, cells were cultured in 15 cm dishes, treated with the indicated drugs or vehicle for 12 hr, washed twice with cold PBS containing 100 μg/ml cycloheximide, collected, and lysed in 450 μl of hypotonic buffer (5 mM Tris-HCl [pH 7.5], 2.5 mM $MgCl_2$, 1.5 mM KCl, 100 μg/ml cycloheximide, 2 mM DTT, 0.5% Triton X-100, and 0.5% sodium deoxycholate). Lysates were

loaded onto 10%–50% (wt/vol) sucrose density gradients (20 mM HEPES-KOH [pH 7.6], 100 mM KCl, and 5 mM $MgCl_2$) and centrifuged at 36,000 rpm (SW 40 Ti rotor, Beckman Coulter, Inc.) for 2 hr at 4°C. Gradients were fractionated and optical density at 254 nm was continuously recorded using an ISCO fractionator (Teledyne ISCO). RNA from each fraction and input was isolated using TRIzol (Invitrogen) according to the manufacturer's instructions. RT-sqPCR reactions were carried out using SuperScript III First-Strand Synthesis System (Invitrogen) and iQ SYBR Green Supermix (Bio-Rad) according to the manufacturers' instructions. The list of primers is provided in Table S3.

Cell Lysis, Western Blotting, and Cap (m^7GDP) Pull-Down Assay

Cells were lysed in lysis buffer (50 mM Tris-HCl [pH 7.5], 150 mM NaCl, 1 mM EDTA, 1% NP-40, Roche complete protease inhibitor cocktail). Protein concentrations were estimated with the Bio-Rad protein assay, and western blotting was carried out as described (Dowling et al., 2010). The information about antibodies is described in Supplemental Experimental Procedures. Cap pull-down assay was carried out as described (Dowling et al., 2010). Briefly, cells were lysed by three freeze-thaw cycles in the cap pull-down buffer (50 mM HEPES-KOH [pH 7.5], 150 mM KCl, 1 mM EDTA, 2 mM DTT, and 0.2% Tween-20) containing protease inhibitors. Protein extract (1 mg) was incubated for 2 hr at 4°C with m^7GDP-agarose beads. After incubation, beads were washed five times with the cap pull-down buffer and eluted by boiling in the presence of 1× sample buffer for 5 min. m^7GDP-bound proteins were visualized by western blotting.

Respiration Assay

The respiration assay was carried out as described (Eichner et al., 2010). Briefly, cells were cultured in 10 cm or 15 cm dishes, treated with the indicated drugs or vehicle for 12 hr, trypsinized, and resuspended in PBS supplemented with 25 mM glucose, 1 mM pyruvate, and 2% BSA. A TC10 automated cell counter assessed total cell count and cell viability via Trypan blue dye exclusion (Bio-Rad). A total of 2.0×10^6 cells were placed in the chamber of a Clark-type oxygen electrode, and cellular respiration was measured. Oligomycin-sensitive respiration represents ATP turnover. Oligomycin-insensitive respiration represents proton leak. Myxothiazol was added to quantify nonmitochondrial respiration. In all experiments performed, nonmitochondrial respiration was undetectable.

Mitochondrial DNA Quantification and Mitochondrial Mass Quantification

The mitochondrial DNA quantification assay was carried out as described (Cunningham et al., 2007). Briefly, cells were treated with the indicated drugs or vehicle for 24 hr. Genomic and mitochondrial DNA was extracted using DNeasy Blood and Tissue kit (QIAGEN). Genomic and mitochondrial DNA was quantified by qPCR using iQ SYBR Green Supermix (Bio-Rad). The list of primers is provided in Table S3.

For the quantification of mitochondrial mass, drug-treated cells were trypsinized, washed with PBS twice, and stained with 10% FBS-DMEM containing 500 nM MitoTracker Deep Red FM (Invitrogen) for 30 min at 37°C. MitoTracker fluorescence intensities were analyzed by FACS (BD). Relative mean fluorescence intensities were calculated by FlowJo (Tree Star, Inc.) and used to determine mitochondrial mass.

LC-MS, NMR, and Mass Isotopomer Distribution Analysis by GC-MS

LC-MS and NMR analyses and mass isotopomer distribution analysis are described in Supplemental Experimental Procedures. Briefly, for LC-MS and NMR analyses, cells were treated with vehicle or asTORi for 12 hr, and metabolites were extracted and analyzed by LC-MS or NMR. For mass isotopomer distribution analysis, cell were treated with vehicle or asTORi for 12 hr and washed with PBS, and media containing 10% dialyzed FBS and 5.55 mM D [U-^{13}C]glucose (Cambridge Isotope Laboratories) was added for 30 min. Cells were washed with ice-cold normal saline solution, and metabolites were extracted and analyzed by GC-MS.

In Vivo Metabolic Studies

In vivo metabolic studies are described in Supplemental Experimental Procedures. Briefly, each mouse was housed in a separate cage and maintained on a 12 hr dark-light cycle with access to food and water ad libitum. For asTORi treatment, Ink1341 was formulated in 5% NMP (1-methyl-2-pyrrolidinone), 15% polyvinylpyrrolidone K30, and 80% water and administrated intraperitoneally at 3 mg/kg body weight daily for 2 weeks. Oxygen consumption, locomotor activity, and heat production were determined with an Oxymax-CLAMS system (Columbus Instruments) according to the manufacturer's instruction. All mouse experiments were carried out in accordance with the guidelines for animal use issued by the McGill University Animal Care Committee.

Statistical Analysis

All values represent mean ± standard deviation (SD) of three independent experiments (unless otherwise indicated). Differences between groups were examined for statistical significance using Student's t test (two-tailed distribution with two-sample equal variance). We considered a p value of < 0.05 statistically significant.

SUPPLEMENTAL INFORMATION

Supplemental Information includes seven figures, three tables, and Supplemental Experimental Procedures and can be found with this article online at http://dx.doi.org/10.1016/j.cmet.2013.10.001.

ACKNOWLEDGMENTS

We thank Y. Liu for providing PP242 and Ink1341, M.C. Gingras for technical assistance with metabolic cages, V. Henderson for editing the manuscript, and C. Lister, P. Kirk, A. Sylvestre, S. Perreault, and I. Harvey for assistance. Research was supported by a Terry Fox Research Institute team grant (TFF-116128) to N.S., I.T., M.P., D.A., A.P., and J.S-P. and grants from the Canadian Institutes of Health Research (CIHR MOP-7214 to N.S.; MOP-115195 to I.T.; MOP-106603 to J.S-P.) and the Canadian Cancer Society Research Institute (CCSRI 16208 to N.S.). I.T. is a recipient of CIHR New Investigator Salary Award. J.S-P. is an FRSQ scholar. M.M. is a recipient of a CIHR-funded Chemical Biology Postdoctoral fellowship and Canadian Diabetes Association Postdoctoral fellowship. S.-P.G. is supported by a Canderel fellowship.

Goodman Cancer Research Centre Metabolomics Core Facility is supported by the Canada Foundation of Innovation, The Dr. John R. and Clara M. Fraser Memorial Trust, the Terry Fox Foundation, the Canadian Institutes of Health Research, and McGill University. The Québec/Eastern Canada High Field NMR Facility is supported by the Natural Sciences and Engineering Research Council of Canada, the Canada Foundation for Innovation, the Québec ministère de la recherche en science et technologie, and McGill University.

REFERENCES

Alain, T., Morita, M., Fonseca, B.D., Yanagiya, A., Siddiqui, N., Bhat, M., Zammit, D., Marcus, V., Metrakos, P., Voyer, L.A., et al. (2012). eIF4E/4E-BP ratio predicts the efficacy of mTOR targeted therapies. Cancer Res. *72*, 6468–6476.

Anderson, P. (2010). Post-transcriptional regulons coordinate the initiation and resolution of inflammation. Nat. Rev. Immunol. *10*, 24–35.

Avdulov, S., Li, S., Michalek, V., Burrichter, D., Peterson, M., Perlman, D.M., Manivel, J.C., Sonenberg, N., Yee, D., Bitterman, P.B., and Polunovsky, V.A. (2004). Activation of translation complex eIF4F is essential for the genesis and maintenance of the malignant phenotype in human mammary epithelial cells. Cancer Cell *5*, 553–563.

Banerjee, P., Ahmad, M.F., Grove, J.R., Kozlosky, C., Price, D.J., and Avruch, J. (1990). Molecular structure of a major insulin/mitogen-activated 70-kDa S6 protein kinase. Proc. Natl. Acad. Sci. USA *87*, 8550–8554.

Benjamin, D., Colombi, M., Moroni, C., and Hall, M.N. (2011). Rapamycin passes the torch: a new generation of mTOR inhibitors. Nat. Rev. Drug Discov. *10*, 868–880.

Bentzinger, C.F., Romanino, K., Cloëtta, D., Lin, S., Mascarenhas, J.B., Oliveri, F., Xia, J., Casanova, E., Costa, C.F., Brink, M., et al. (2008). Skeletal muscle-specific ablation of raptor, but not of rictor, causes metabolic changes and results in muscle dystrophy. Cell Metab. *8*, 411–424.

Betz, C., Stracka, D., Prescianotto-Baschong, C., Frieden, M., Demaurex, N., and Hall, M.N. (2013). Feature Article: mTOR complex 2-Akt signaling at mitochondria-associated endoplasmic reticulum membranes (MAM) regulates mitochondrial physiology. Proc. Natl. Acad. Sci. USA *110*, 12526–12534.

Blättler, S.M., Verdeguer, F., Liesa, M., Cunningham, J.T., Vogel, R.O., Chim, H., Liu, H., Romanino, K., Shirihai, O.S., Vazquez, F., et al. (2012). Defective mitochondrial morphology and bioenergetic function in mice lacking the transcription factor Yin Yang 1 in skeletal muscle. Mol. Cell. Biol. *32*, 3333–3346.

Bonawitz, N.D., Clayton, D.A., and Shadel, G.S. (2006). Initiation and beyond: multiple functions of the human mitochondrial transcription machinery. Mol. Cell *24*, 813–825.

Buttgereit, F., and Brand, M.D. (1995). A hierarchy of ATP-consuming processes in mammalian cells. Biochem. J. *312*, 163–167.

Conn, C.S., and Qian, S.B. (2013). Nutrient signaling in protein homeostasis: an increase in quantity at the expense of quality. Sci. Signal. *6*, ra24.

Cunningham, J.T., Rodgers, J.T., Arlow, D.H., Vazquez, F., Mootha, V.K., and Puigserver, P. (2007). mTOR controls mitochondrial oxidative function through a YY1-PGC-1alpha transcriptional complex. Nature *450*, 736–740.

Dorrello, N.V., Peschiaroli, A., Guardavaccaro, D., Colburn, N.H., Sherman, N.E., and Pagano, M. (2006). S6K1- and betaTRCP-mediated degradation of PDCD4 promotes protein translation and cell growth. Science *314*, 467–471.

Dowling, R.J., Topisirovic, I., Alain, T., Bidinosti, M., Fonseca, B.D., Petroulakis, E., Wang, X., Larsson, O., Selvaraj, A., Liu, Y., et al. (2010). mTORC1-mediated cell proliferation, but not cell growth, controlled by the 4E-BPs. Science *328*, 1172–1176.

Düvel, K., Yecies, J.L., Menon, S., Raman, P., Lipovsky, A.I., Souza, A.L., Triantafellow, E., Ma, Q., Gorski, R., Cleaver, S., et al. (2010). Activation of a metabolic gene regulatory network downstream of mTOR complex 1. Mol. Cell *39*, 171–183.

Eichner, L.J., Perry, M.C., Dufour, C.R., Bertos, N., Park, M., St-Pierre, J., and Giguère, V. (2010). miR-378(*) mediates metabolic shift in breast cancer cells via the PGC-1β/ERRγ transcriptional pathway. Cell Metab. *12*, 352–361.

Fleming, A., Noda, T., Yoshimori, T., and Rubinsztein, D.C. (2011). Chemical modulators of autophagy as biological probes and potential therapeutics. Nat. Chem. Biol. *7*, 9–17.

Fornuskova, D., Stiburek, L., Wenchich, L., Vinsova, K., Hansikova, H., and Zeman, J. (2010). Novel insights into the assembly and function of human nuclear-encoded cytochrome c oxidase subunits 4, 5a, 6a, 7a and 7b. Biochem. J. *428*, 363–374.

García-Martínez, J.M., and Alessi, D.R. (2008). mTOR complex 2 (mTORC2) controls hydrophobic motif phosphorylation and activation of serum- and glucocorticoid-induced protein kinase 1 (SGK1). Biochem. J. *416*, 375–385.

Gentleman, R.C., Carey, V.J., Bates, D.M., Bolstad, B., Dettling, M., Dudoit, S., Ellis, B., Gautier, L., Ge, Y., Gentry, J., et al. (2004). Bioconductor: open software development for computational biology and bioinformatics. Genome Biol. *5*, R80.

Gingras, A.C., Gygi, S.P., Raught, B., Polakiewicz, R.D., Abraham, R.T., Hoekstra, M.F., Aebersold, R., and Sonenberg, N. (1999). Regulation of 4E-BP1 phosphorylation: a novel two-step mechanism. Genes Dev. *13*, 1422–1437.

Gingras, A.C., Raught, B., Gygi, S.P., Niedzwiecka, A., Miron, M., Burley, S.K., Polakiewicz, R.D., Wyslouch-Cieszynska, A., Aebersold, R., and Sonenberg, N. (2001). Hierarchical phosphorylation of the translation inhibitor 4E-BP1. Genes Dev. *15*, 2852–2864.

Goo, C.K., Lim, H.Y., Ho, Q.S., Too, H.P., Clement, M.V., and Wong, K.P. (2012). PTEN/Akt signaling controls mitochondrial respiratory capacity through 4E-BP1. PLoS ONE *7*, e45806.

Hagiwara, A., Cornu, M., Cybulski, N., Polak, P., Betz, C., Trapani, F., Terracciano, L., Heim, M.H., Rüegg, M.A., and Hall, M.N. (2012). Hepatic mTORC2 activates glycolysis and lipogenesis through Akt, glucokinase, and SREBP1c. Cell Metab. *15*, 725–738.

Hara, K., Maruki, Y., Long, X., Yoshino, K., Oshiro, N., Hidayat, S., Tokunaga, C., Avruch, J., and Yonezawa, K. (2002). Raptor, a binding partner of target of rapamycin (TOR), mediates TOR action. Cell *110*, 177–189.

Hoffmann, J., Sokolova, L., Preiss, L., Hicks, D.B., Krulwich, T.A., Morgner, N., Wittig, I., Schägger, H., Meier, T., and Brutschy, B. (2010). ATP synthases: cellular nanomotors characterized by LILBID mass spectrometry. Phys. Chem. Chem. Phys. *12*, 13375–13382.

Hsieh, A.C., Liu, Y., Edlind, M.P., Ingolia, N.T., Janes, M.R., Sher, A., Shi, E.Y., Stumpf, C.R., Christensen, C., Bonham, M.J., et al. (2012). The translational landscape of mTOR signalling steers cancer initiation and metastasis. Nature *485*, 55–61.

Ikenoue, T., Inoki, K., Yang, Q., Zhou, X., and Guan, K.L. (2008). Essential function of TORC2 in PKC and Akt turn motif phosphorylation, maturation and signalling. EMBO J. *27*, 1919–1931.

Inoki, K., Li, Y., Xu, T., and Guan, K.L. (2003). Rheb GTPase is a direct target of TSC2 GAP activity and regulates mTOR signaling. Genes Dev. *17*, 1829–1834.

Jacinto, E., Loewith, R., Schmidt, A., Lin, S., Rüegg, M.A., Hall, A., and Hall, M.N. (2004). Mammalian TOR complex 2 controls the actin cytoskeleton and is rapamycin insensitive. Nat. Cell Biol. *6*, 1122–1128.

Kim, D.H., Sarbassov, D.D., Ali, S.M., King, J.E., Latek, R.R., Erdjument-Bromage, H., Tempst, P., and Sabatini, D.M. (2002). mTOR interacts with raptor to form a nutrient-sensitive complex that signals to the cell growth machinery. Cell *110*, 163–175.

Kozma, S.C., Ferrari, S., Bassand, P., Siegmann, M., Totty, N., and Thomas, G. (1990). Cloning of the mitogen-activated S6 kinase from rat liver reveals an enzyme of the second messenger subfamily. Proc. Natl. Acad. Sci. USA *87*, 7365–7369.

Laplante, M., and Sabatini, D.M. (2012). mTOR signaling in growth control and disease. Cell *149*, 274–293.

Larsson, O., Sonenberg, N., and Nadon, R. (2010). Identification of differential translation in genome wide studies. Proc. Natl. Acad. Sci. USA *107*, 21487–21492.

Larsson, O., Sonenberg, N., and Nadon, R. (2011). anota: Analysis of differential translation in genome-wide studies. Bioinformatics *27*, 1440–1441.

Larsson, O., Morita, M., Topisirovic, I., Alain, T., Blouin, M.J., Pollak, M., and Sonenberg, N. (2012). Distinct perturbation of the translatome by the antidiabetic drug metformin. Proc. Natl. Acad. Sci. USA *109*, 8977–8982.

Lazaris-Karatzas, A., Montine, K.S., and Sonenberg, N. (1990). Malignant transformation by a eukaryotic initiation factor subunit that binds to mRNA 5′ cap. Nature *345*, 544–547.

Lehman, J.J., Barger, P.M., Kovacs, A., Saffitz, J.E., Medeiros, D.M., and Kelly, D.P. (2000). Peroxisome proliferator-activated receptor gamma coactivator-1 promotes cardiac mitochondrial biogenesis. J. Clin. Invest. *106*, 847–856.

Luo, W., Friedman, M.S., Shedden, K., Hankenson, K.D., and Woolf, P.J. (2009). GAGE: generally applicable gene set enrichment for pathway analysis. BMC Bioinformatics *10*, 161.

Nanchen, A., Fuhrer, T., and Sauer, U. (2007). Determination of metabolic flux ratios from 13C-experiments and gas chromatography-mass spectrometry data: protocol and principles. Methods Mol. Biol. *358*, 177–197.

Pause, A., Belsham, G.J., Gingras, A.C., Donzé, O., Lin, T.A., Lawrence, J.C., Jr., and Sonenberg, N. (1994). Insulin-dependent stimulation of protein synthesis by phosphorylation of a regulator of 5′-cap function. Nature *371*, 762–767.

Polak, P., Cybulski, N., Feige, J.N., Auwerx, J., Rüegg, M.A., and Hall, M.N. (2008). Adipose-specific knockout of raptor results in lean mice with enhanced mitochondrial respiration. Cell Metab. *8*, 399–410.

Porstmann, T., Santos, C.R., Griffiths, B., Cully, M., Wu, M., Leevers, S., Griffiths, J.R., Chung, Y.L., and Schulze, A. (2008). SREBP activity is regulated

by mTORC1 and contributes to Akt-dependent cell growth. Cell Metab. *8*, 224–236.

Rolfe, D.F., and Brown, G.C. (1997). Cellular energy utilization and molecular origin of standard metabolic rate in mammals. Physiol. Rev. *77*, 731–758.

Roux, P.P., and Topisirovic, I. (2012). Regulation of mRNA translation by signaling pathways. Cold Spring Harb. Perspect. Biol. *4*, a012252.

Ruggero, D., Montanaro, L., Ma, L., Xu, W., Londei, P., Cordon-Cardo, C., and Pandolfi, P.P. (2004). The translation factor eIF-4E promotes tumor formation and cooperates with c-Myc in lymphomagenesis. Nat. Med. *10*, 484–486.

Sarbassov, D.D., Ali, S.M., Kim, D.H., Guertin, D.A., Latek, R.R., Erdjument-Bromage, H., Tempst, P., and Sabatini, D.M. (2004). Rictor, a novel binding partner of mTOR, defines a rapamycin-insensitive and raptor-independent pathway that regulates the cytoskeleton. Curr. Biol. *14*, 1296–1302.

Sarbassov, D.D., Guertin, D.A., Ali, S.M., and Sabatini, D.M. (2005). Phosphorylation and regulation of Akt/PKB by the rictor-mTOR complex. Science *307*, 1098–1101.

Schieke, S.M., Phillips, D., McCoy, J.P., Jr., Aponte, A.M., Shen, R.F., Balaban, R.S., and Finkel, T. (2006). The mammalian target of rapamycin (mTOR) pathway regulates mitochondrial oxygen consumption and oxidative capacity. J. Biol. Chem. *281*, 27643–27652.

Shahbazian, D., Roux, P.P., Mieulet, V., Cohen, M.S., Raught, B., Taunton, J., Hershey, J.W., Blenis, J., Pende, M., and Sonenberg, N. (2006). The mTOR/PI3K and MAPK pathways converge on eIF4B to control its phosphorylation and activity. EMBO J. *25*, 2781–2791.

She, P., Reid, T.M., Bronson, S.K., Vary, T.C., Hajnal, A., Lynch, C.J., and Hutson, S.M. (2007). Disruption of BCATm in mice leads to increased energy expenditure associated with the activation of a futile protein turnover cycle. Cell Metab. *6*, 181–194.

St-Pierre, J., Lin, J., Krauss, S., Tarr, P.T., Yang, R., Newgard, C.B., and Spiegelman, B.M. (2003). Bioenergetic analysis of peroxisome proliferator-activated receptor gamma coactivators 1alpha and 1beta (PGC-1alpha and PGC-1beta) in muscle cells. J. Biol. Chem. *278*, 26597–26603.

Sun, J., Conn, C.S., Han, Y., Yeung, V., and Qian, S.B. (2011). PI3K-mTORC1 attenuates stress response by inhibiting cap-independent Hsp70 translation. J. Biol. Chem. *286*, 6791–6800.

Tee, A.R., Manning, B.D., Roux, P.P., Cantley, L.C., and Blenis, J. (2003). Tuberous sclerosis complex gene products, Tuberin and Hamartin, control mTOR signaling by acting as a GTPase-activating protein complex toward Rheb. Curr. Biol. *13*, 1259–1268.

Thoreen, C.C., Kang, S.A., Chang, J.W., Liu, Q., Zhang, J., Gao, Y., Reichling, L.J., Sim, T., Sabatini, D.M., and Gray, N.S. (2009). An ATP-competitive mammalian target of rapamycin inhibitor reveals rapamycin-resistant functions of mTORC1. J. Biol. Chem. *284*, 8023–8032.

Thoreen, C.C., Chantranupong, L., Keys, H.R., Wang, T., Gray, N.S., and Sabatini, D.M. (2012). A unifying model for mTORC1-mediated regulation of mRNA translation. Nature *485*, 109–113.

Vander Heiden, M.G., Cantley, L.C., and Thompson, C.B. (2009). Understanding the Warburg effect: the metabolic requirements of cell proliferation. Science *324*, 1029–1033.

Ward, P.S., and Thompson, C.B. (2012). Metabolic reprogramming: a cancer hallmark even warburg did not anticipate. Cancer Cell *21*, 297–308.

Wendel, H.G., De Stanchina, E., Fridman, J.S., Malina, A., Ray, S., Kogan, S., Cordon-Cardo, C., Pelletier, J., and Lowe, S.W. (2004). Survival signalling by Akt and eIF4E in oncogenesis and cancer therapy. Nature *428*, 332–337.

Yecies, J.L., and Manning, B.D. (2011). mTOR links oncogenic signaling to tumor cell metabolism. J. Mol. Med. *89*, 221–228.

Yu, K., Toral-Barza, L., Shi, C., Zhang, W.G., Lucas, J., Shor, B., Kim, J., Verheijen, J., Curran, K., Malwitz, D.J., et al. (2009). Biochemical, cellular, and in vivo activity of novel ATP-competitive and selective inhibitors of the mammalian target of rapamycin. Cancer Res. *69*, 6232–6240.

Yuan, M., Pino, E., Wu, L., Kacergis, M., and Soukas, A.A. (2012). Identification of Akt-independent regulation of hepatic lipogenesis by mammalian target of rapamycin (mTOR) complex 2. J. Biol. Chem. *287*, 29579–29588.

Zhang, H., Cicchetti, G., Onda, H., Koon, H.B., Asrican, K., Bajraszewski, N., Vazquez, F., Carpenter, C.L., and Kwiatkowski, D.J. (2003). Loss of Tsc1/Tsc2 activates mTOR and disrupts PI3K-Akt signaling through downregulation of PDGFR. J. Clin. Invest. *112*, 1223–1233.

Zid, B.M., Rogers, A.N., Katewa, S.D., Vargas, M.A., Kolipinski, M.C., Lu, T.A., Benzer, S., and Kapahi, P. (2009). 4E-BP extends lifespan upon dietary restriction by enhancing mitochondrial activity in Drosophila. Cell *139*, 149–160.

Zoncu, R., Efeyan, A., and Sabatini, D.M. (2011). mTOR: from growth signal integration to cancer, diabetes and ageing. Nat. Rev. Mol. Cell Biol. *12*, 21–35.